Fabrication of ordered Fe Ni nitride film with equiatomic Fe/Ni ratio

doi: 10.7567/JJAP.57.058004

Japanese Journal of Applied Physics

The Japan Society of Applied Physics

BRIEF NOTES • OPEN ACCESS

Fabrication of ordered Fe–Ni nitride film with equiatomic Fe/Ni ratio

OPEN ACCESS

Japanese Journal of Applied Physics **57**, 058004 (2018)

https://doi.org/10.7567/JJAP.57.058004

BRIEF NOTE

Fabrication of ordered Fe–Ni nitride film with equiatomic Fe/Ni ratio

Fumiya Takata, Keita Ito, and Takashi Suemasu*

Institute of Applied Physics, Graduate School of Pure and Applied Sciences, University of Tsukuba, Tsukuba, Ibaraki 305-8573, Japan

*E-mail: suemasu@bk.tsukuba.ac.jp

Received January 24, 2018; accepted March 16, 2018; published online April 16, 2018

We successfully grew a single-phase tetragonal FeNiN film with an equiatomic ratio of Fe, Ni, and N on a MgO(001) substrate by molecular beam epitaxy. We then demonstrated the formation of Fe_2Ni_2N films by extracting N atoms from the FeNiN film. These results suggested that Fe and Ni atoms in the Fe_2Ni_2N film were $L1_0$-ordered along the film plane direction because of the *a*-axis orientation growth of the FeNiN film on the MgO(001) substrate. © 2018 The Japan Society of Applied Physics

Fe–Ni nitrides have attracted much interest owing to the rich variety in their magnetic and transport properties.[1–10] In particular, anti-perovskite type cubic Fe–Ni nitride $Fe_{4-x}Ni_xN$, where the metallic atoms form an fcc lattice with a N atom positioned at a body-center position, have been extensively studied not only for magnetic materials but also for spintronic applications. For example, Fe_4N has been theoretically predicted to have a very large negative spin-polarization of electrical conductivity,[11] and its high spin-polarization has been experimentally demonstrated by the point-contact Andreev reflection technique and the tunneling magnetoresistance effect.[12,13] It is reported that substitution of Ni for Fe atoms improves the chemical stability and mechanical ductility of these materials,[6,7] and modifies their magnetic and electronic structure.[5] The saturation magnetization (M_S) and lattice constant tend to decrease with increasing the Ni content.[8] According to a Mössbauer study and first-principle calculations, Ni atoms likely occupy corner sites.[9,10] Recently, our group and another showed that $FeNi_3N$ has a larger negative spin-polarization of its density of states at the Fermi level than that of Fe_4N, and was thus suggested to be a high spin-polarized material.[14,15] Previously, we succeeded in growing $Fe_{4-x}Ni_xN$ ($x = 0$, 1, 3, and 4) epitaxial films on a $SrTiO_3$(001) substrate by molecular beam epitaxy (MBE), and investigated their structure, magnetic properties, and magnetotransport properties in detail.[15–17]

Another Fe–Ni nitride phase with an equiatomic ratio of Fe, Ni, and N, namely FeNiN, was discovered by Arnott and Wold during the nitriding process of Fe_2Ni_2N powders. The crystal structure was determined to be face-centered tetragonal (space group: $P4/mmm$) with lattice parameters of a (in-plane) = 4.002 Å, c (out-of-plane) = 3.713 Å, and c/a = 0.928 as shown in Fig. 1(a).[18] A notable feature of this phase is the atomic ordering of Fe and Ni atoms, namely, Fe and Ni monolayers alternately stack along the *c*-axis direction, which form a so-called $L1_0$ structure, with N atoms located side by side with Fe atoms. Quite recently, Goto et al. pointed out that FeNiN is an important intermediate phase for obtaining single-phase $L1_0$-FeNi,[19] which is a promising material from the perspective of both rare-earth free permanent magnets and ferromagnetic films with perpendicular magnetic anisotropy (PMA). These phenomena can be attributed to its large uniaxial magnetic anisotropy appearing in the *c*-axis direction.[20] According to Goto et al., N atoms diffuse out without disturbing the atomic ordering of the Fe and Ni atoms during the denitriding process, and therefore highly ordered $L1_0$-FeNi alloy powder can be obtained. These interesting phenomena motivated us to fabricate FeNiN epitaxial films and then extract N atoms from the FeNiN film. There have been no reports thus far on the formation of FeNiN films. In this study, we grew FeNiN films, and demonstrated the fabrication of a Fe_2Ni_2N film, as shown in Fig. 1(b), by extracting N atoms from FeNiN films.

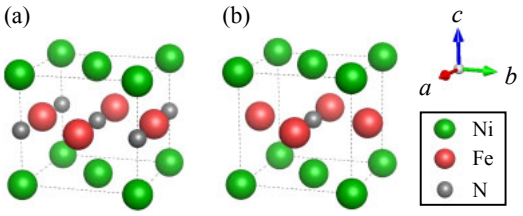

Fig. 1. (Color online) Crystal structure of (a) FeNiN and (b) Fe_2Ni_2N.

40-nm thick FeNiN films were grown on MgO(001) single-crystal substrates by MBE with the use of solid Fe and Ni sources, and a radio-frequency N_2 plasma. We followed the same growth condition as that for $Fe_{4-x}Ni_xN$ films,[15] and controlled the crucibles temperatures of Fe and Ni, setting their atomic ratio to be 1 : 1. The total deposition rate was set at 0.5 nm/min, which was half that of $Fe_{4-x}Ni_xN$ films. The substrate temperature (T_S) was varied from 200 to 450 °C. A 3 nm-thick SiO_2 capping layer was in situ deposited by sputtering. N extraction was performed by annealing under vacuum for 30 min at an annealing temperature in the range of T_A of 300–400 °C. The crystalline qualities and structures were characterized by reflection high-energy electron diffraction (RHEED), out-of-plane (2θ–ω) X-ray diffraction (XRD), and in-plane ($2\theta_\chi$–ϕ) XRD measurements with Cu-Kα radiation. The magnetic properties were measured with a vibrating sample magnetometer at room temperature.

Figure 2 shows the out-of-plane and in-plane XRD profiles and RHEED patterns of the samples grown at T_S = 200, 300, and 450 °C. The incident electron beam was set along the MgO[100] azimuth. When the T_S were 200 and 300 °C, XRD peaks originating only from FeNiN were observed. The (h00)-oriented peaks were confirmed in the out-of-plane XRD, whereas (0k0)- and (00l)-oriented peaks appeared in the in-plane XRD profiles when the X-ray scattering vector ($\boldsymbol{Q}$) was set to MgO[200]. These results verified the epitaxial

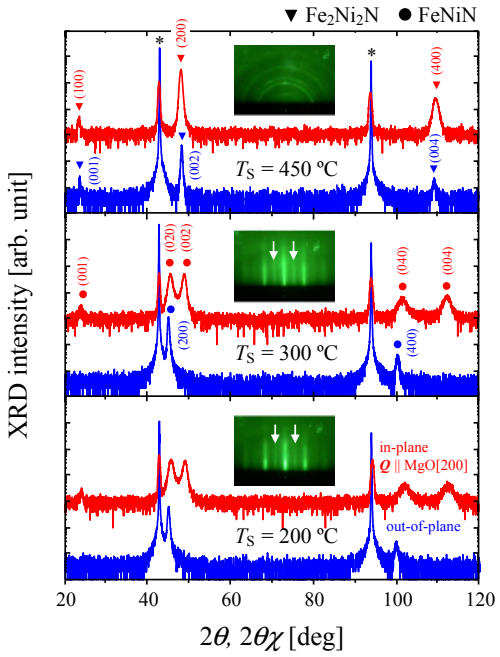

Fig. 2. (Color online) Out-of-plane (blue, lower) and in-plane XRD (red, upper) and RHEED patterns of samples grown at $T_S = 200$, 300, and 450 °C. Asterisks indicate diffraction peaks from the substrate.

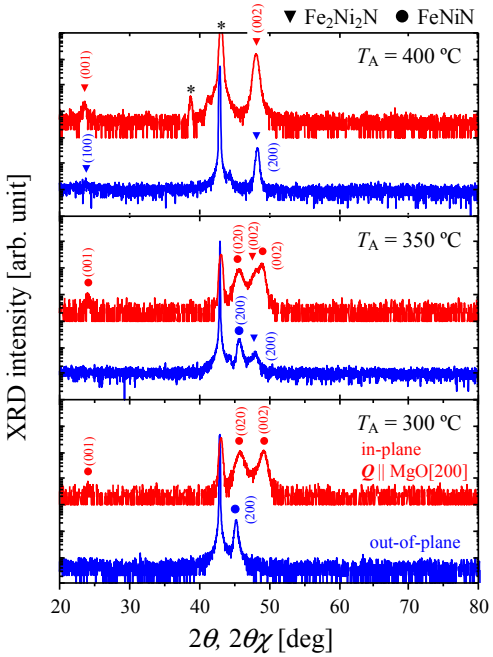

Fig. 3. (Color online) Out-of-plane (blue, lower) and in-plane XRD (red, upper) patterns of FeNiN film after annealed at $T_A = 300$, 350, and 400 °C. Asterisks indicate diffraction peaks from the substrate.

growth of single-phase FeNiN films on MgO(001) with an epitaxial relationship of FeNiN[001](100) ∥ MgO[100](001) and FeNiN[010](100) ∥ MgO[100](001). An FeNiN film consists of two variants, whose c-axis was in-plane and rotated around the film normal by 90° each other. However, this epitaxial relationship is different from our prediction that the favored epitaxial relationship would be FeNiN[100](001) ∥ MgO[100](001), i.e., a cube-on-cube relationship, with the smallest lattice mismatch of approximately −5%. The RHEED results clearly show streaky patterns together with superlattice streaks, as indicated by arrows in Fig. 2, owing to a long-range order of the N atoms. The lattice constants were calculated to be $a = 4.01$ Å, $c = 3.71$ Å, and $c/a = 0.925$, which are close to those reported.[18] For the sample grown at $T_S = 450$ °C, both the out-of-plane and in-plane XRD patterns indicate the c-axis-oriented epitaxial growth of Fe_2Ni_2N; however, the RHEED pattern changed from streaky to a ring shape. These results show the coexistence of epitaxial Fe_2Ni_2N grains and non-epitaxial ones in the grown film. The superlattice diffractions of the Fe_2Ni_2N(001) and (100) indicated a long-range order of N atoms at body-center sites.[15] The order parameter of N body-center site (S_N) was calculated to be 0.77 using the superlattice diffraction of Fe_2Ni_2N(100) and the fundamental diffraction of Fe_2Ni_2N(200).[15] We considered that N atoms diffused from the FeNiN film at elevated T_S to form Fe_2Ni_2N. The obtained Fe_2Ni_2N film had a cubic structure with $a = 3.776$ Å, $c = 3.779$ Å, and $c/a = 1.001$. We note that it was necessary to grow a c-axis oriented FeNiN film to obtain an $L1_0$-FeNi film with PMA through N extraction. Thus, further studies on the growth of FeNiN films with c-axis orientation are required in future work.

Next, we attempted to extract N atoms from the FeNiN film. We selected FeNiN films grown at $T_S = 200$ °C based on the XRD results shown in Fig. 2. Figure 3 shows the out-of-plane (2θ–ω) and in-plane ($2\theta_\chi$–ϕ) XRD patterns obtained after annealing at $T_A = 300$, 350, and 400 °C. No notable change was found at $T_A = 300$ °C. When T_A was increased to 350 °C, we noted diffraction peaks from both Fe_2Ni_2N and FeNiN phases. When T_A was increased further to 400 °C, a single-phase Fe_2Ni_2N film was obtained. The S_N was determined to be 0.74, which was almost the same as Fe_2Ni_2N film shown in Fig. 2. This means that we succeeded in extracting approximately 50% of the N atoms from the FeNiN film by a simple post-annealing process. We note that the Fe_2Ni_2N film with extracted N atoms featured a tetragonal structure with $a = 3.788$ Å, $c = 3.768$ Å, and $c/a = 0.995$, which was different from the cubic one directly grown at $T_S = 450$ °C, as shown in Fig. 2. We presume that this tetragonal distortion indicates atomic ordering in the Fe_2Ni_2N film because the $L1_0$-FeNi alloy also has a small tetragonal distortion of $c/a \sim 1.007$.[20]

Figures 4(a) and 4(b) show the hysteresis curves of Fe_2Ni_2N films obtained by direct MBE growth at $T_S = 450$ °C and by extracting N atoms at $T_A = 400$ °C under vacuum from the FeNiN film grown at $T_S = 200$ °C, respectively. The magnetic fields were applied parallel ([100]) and perpendicular ([001]) to the substrate. In-plane easy magnetization with $M_S = 700 \pm 100$ emu/cm^3 was confirmed in both films. Compared with Fig. 4(a), a larger magnetic field was required to saturate the magnetization perpendicular to the film plane in Fig. 4(b). This increase of the perpendicular saturation field of the Fe_2Ni_2N film also probably comes from atomic ordering. In our film, the $L1_0$ atomic ordering of the Fe and Ni atoms likely occurred parallel to the film plane, because the FeNiN film was grown with a-axis orientation. Hence, we assumed that the atomic ordering of Fe and Ni atoms in Fe_2Ni_2N enhanced the uniaxial magnetic anisotropy along the stacking direction of the Fe and Ni monolayers. If we can acquire c-axis oriented FeNiN film, uniaxial magnetic

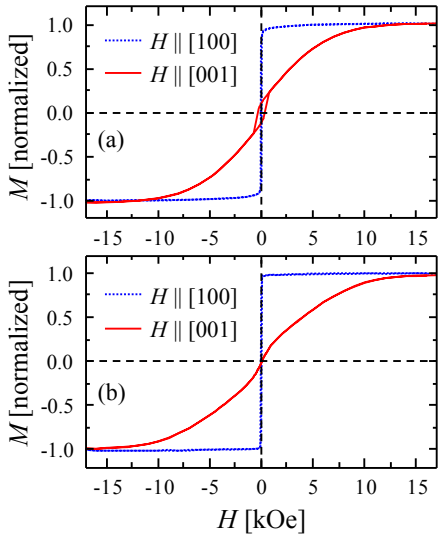

Fig. 4. (Color online) Hysteresis curves of Fe_2Ni_2N films obtained by (a) direct growth at $T_S = 450\,°C$ and (b) by N extraction from FeNiN film.

anisotropy of Fe_2Ni_2N films increases in perpendicular to the film plane. $L1_0$ ordering of metallic atoms in anti-perovskite type ferromagnetic nitrides has a possibility to show PMA. We believe that this study could also make a major contribution to the formation of $L1_0$-FeNi films by extracting 100% of the N atoms from FeNiN films.

In summary, we achieved epitaxial growth of single-phase FeNiN films on a MgO(001) substrate by MBE and then obtained atomically ordered Fe_2Ni_2N films by extracting N atoms. The FeNiN films were grown with *a*-axis orientation, and therefore the atomic ordering of Fe and Ni atoms occurred parallel to the film plane. This work contributes to a new technique to form anti-perovskite type ferromagnetic nitrides with an equiatomic ratio of metallic atoms, and the fabrication of high $L1_0$-ordered FeNi films.

Acknowledgement Magnetization measurements were performed with the help of Professor H. Yanagihara of the University of Tsukuba.

1) R. N. Panda and N. S. Gajbhiye, J. Appl. Phys. **86**, 3295 (1999).
2) H. Y. Wang, J. H. S. Hang, W. H. Mao, H. Chen, H. Y. Zhang, Y. J. He, and E. Y. Jiang, J. Appl. Phys. **91**, 1453 (2002).
3) P. Prieto, J. Camarero, N. Sacristan, D. O. Boerma, and J. M. Sanz, Phys. Status Solidi A **203**, 1442 (2006).
4) G. Shirane, W. J. Takei, and S. L. Ruby, Phys. Rev. **126**, 49 (1962).
5) Y. Kong and F. Li, Phys. Rev. B **57**, 970 (1998).
6) S. K. Chen, S. Jin, T. H. Tiefel, Y. F. Hsieh, E. M. Gyorgy, and D. W. Johnson, Jr., J. Appl. Phys. **70**, 6247 (1991).
7) M. Kume, T. Tsujioka, K. Matsuura, Y. Abe, and A. Tasaki, IEEE Trans. Magn. **23**, 3633 (1987).
8) X. G. Diao, A. Y. Takeuchi, F. Garcia, R. B. Scorzelli, and H. R. Rechenberg, J. Appl. Phys. **85**, 4485 (1999).
9) F. Li, J. Yang, D. Xue, and R. Zhou, Appl. Phys. Lett. **66**, 2343 (1995).
10) P. Monachesi, T. Björkman, T. Gasche, and O. Eriksson, Phys. Rev. B **88**, 054420 (2013).
11) S. Kokado, N. Fujima, K. Harigaya, H. Shimizu, and A. Sakuma, Phys. Rev. B **73**, 172410 (2006).
12) A. Narahara, K. Ito, T. Suemasu, Y. K. Takahashi, A. Ranajikanth, and K. Hono, Appl. Phys. Lett. **94**, 202502 (2009).
13) Y. Komasaki, M. Tsunoda, S. Isogami, and M. Takahashi, J. Appl. Phys. **105**, 07C928 (2009).
14) Z. R. Li, W. B. Mi, and H. L. Bai, Comput. Mater. Sci. **142**, 145 (2018).
15) F. Takata, K. Ito, S. Higashikozono, T. Gushi, K. Toko, and T. Suemasu, J. Appl. Phys. **120**, 083907 (2016).
16) F. Takata, K. Kabara, K. Ito, M. Tsunoda, and T. Suemasu, J. Appl. Phys. **121**, 023903 (2017).
17) F. Takata, K. Ito, Y. Takeda, Y. Saitoh, K. Takanashi, A. Kimura, and T. Suemasu, Phys. Rev. Mater. **2**, 024407 (2018).
18) R. J. Arnott and A. Wold, J. Phys. Chem. Solids **15**, 152 (1960).
19) S. Goto, H. Kura, E. Watanabe, Y. Hayashi, H. Yanagihara, Y. Shimada, M. Mizuguchi, K. Takanashi, and E. Kita, Sci. Rep. **7**, 13216 (2017).
20) K. Takanashi, M. Mizugushi, T. Kojima, and T. Tashiro, J. Phys. D **50**, 483002 (2017).